Proceedings of Asia-Pacific Microwave Conference 2006

An Enhancement of Input Impedance Bandwidth of Circular-Disc Loaded Monopole Antenna with Horizontal and Vertical Parasitic Strips

Jae W. Lee*, Kyung K. Kang*, Choon-Sik Cho*, and Jaeheung Kim**

*School of Electronics, Telecommunication and Computer Engineering, Hankuk Aviation University
200-1 Hwajun-Dong, Dukyang-Gu, Goyang, Gyeonggi-Do, 412-791, Korea
**School of Engineering, Intelligent Radio Engineering Center, Information and Communications University
Taejon, 305-732, Korea
E-mail: *jwlee1@hau.ac.kr, *kkkang9@hau.ac.kr, *cscho@hau.ac.kr, **jaeheung@chol.com

ABSTRACT – In this paper, a monopole antenna with a circular disc at the top and parasitic strips around antenna is analytically investigated and simulated using the mode-matching technique and a commercially available software package, CST MW Studio based on FDTD algorithm. Mode-matching technique with boundary conditions are applied to compute the unknown modal coefficients in each region. For the usefulness of mode-matching technique to open boundary, the artificial ground plane is added away from the top-loading disc. Compared results between two methods show that the proper radius and height of parasitic elements can reduce the peak value of input impedance at the resonant frequencies over wide bandwidth without power dissipation due to lossy material used in conventional ways.

Key Words – Monopole antenna, circular disc, parasitic strips

I. INTRODUCTION

Generally, in order to increase the input impedance bandwidth, several techniques, which include loading the circular disk on simple monopole, surrounding the center conductor with high dielectric constant, and attaching the sleeve plate on ground plane, have been investigated by many researchers[1-7]. In addition to that, conventional helical antenna, loop and monopole antenna have been studied with focused on wireless communication systems in relatively high frequency and military telecommunications in a little lower frequency.

In order to apply mode-matching technique and matching boundary conditions in the given structure, the entire structure surrounded by air is separated into several regions by using circular coordinates and artificial ground plane. In [2], the artificial ground plane has been suggested to calculate input impedance of monopole antenna using the mode expansion in each region.

In this paper, a study on the enhancement of input impedance bandwidth of circular-disc loaded monopole antenna is carried out by modifying the distribution of parasitic elements. A detailed dimension and the field representations are rigorously discussed in section II. In section III, the reflection coefficients have been derived in an analytically useful series form by using the mode-matching technique.

II. FIELD REPRESENTATIONS

Consider the scattering geometry with a simple monopole antenna surrounded by parasitic elements as shown in Fig. 1. Inner and outer radii of horizontal parasitic strips are denoted by r_i and r_o, respectively.

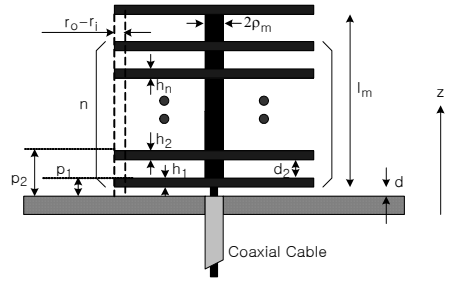

(a)

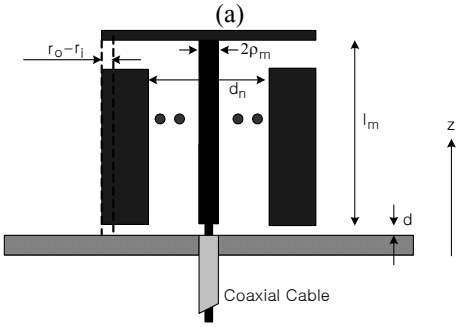

(b)

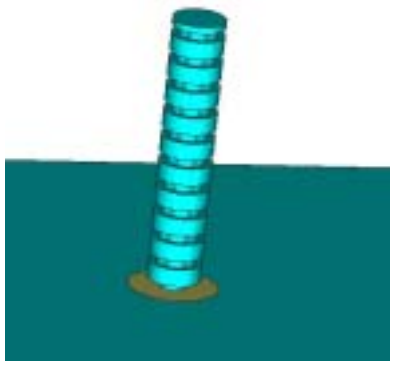

(c)

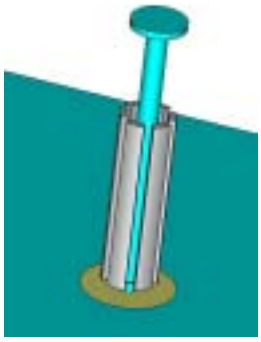

(d)

Fig. 1. The proposed circular-disc loaded monopole antenna (a) with horizontal parasitic strips (b) with vertical parasitic strips (c) 3D-view of (a) (d) 3D-view of (b)

The parasitic strips are aligned with h_i, height of each strip, d_i, the distance between the nearest two strips, and n, the number of parasitic elements. The dimension of ground plane is assumed to be $80[mm]\times 80[mm]$ for the simulation of infinite ground plane in a commercially available software. Moreover, the radius of circular-disc composing main radiator and the length between the feeding point and circular disc are ρ_m and l_m, respectively. For a delta-gap source excitation, the parameter d means the length between the coaxial cable and monopole antenna. For a convenience of computational calculation, limit the general case of Fig. 1 to the case of the number of parasitic element, $N=1$. At this time, the generalized parameters, r_i, r_o and h_i can be rewritten as r_1, b, and h_1.

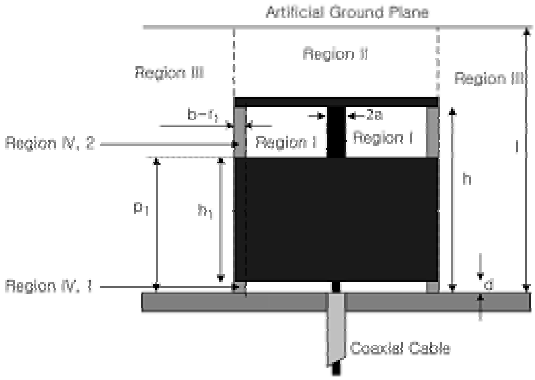

Fig. 2. Region separation for field representations

For the enforcement of matching boundary conditions, the fields in each region are represented as follows.

i) Region (I) $(a \le \rho \le b,\ 0 \le z \le h)$

$$E_z^I(\rho,z)=\frac{1}{j\omega\varepsilon_I}\sum_{n=0}^{n_1}\gamma_n^2[a_nH_0^{(1)}(\gamma_n\rho)+b_nH_0^{(2)}(\gamma_n\rho)]\cos\left(\frac{n\pi z}{h}\right)$$

$$H_\phi^I(\rho,z)=\sum_{n=0}^{n_1}\gamma_n[a_nH_0^{(1)}(\gamma_n\rho)+b_nH_0^{(2)}(\gamma_n\rho)]\cos\left(\frac{n\pi z}{h}\right)$$

ii) Region (II) $(\rho \le b,\ h \le z \le l)$

$$E_z^{II}(\rho,z)=\frac{1}{j\omega\varepsilon_{II}}\sum_{n=0}^{n_2}c_nu_n^2J_0(u_n\rho)\cos\left[\frac{n\pi(z-h)}{q}\right]$$

$$H_\phi^{II}(\rho,z)=\sum_{n=0}^{n_2}c_nu_nJ_1(u_n\rho)\cos\left[\frac{n\pi(z-h)}{q}\right]$$

iii) Region (III) $(b \le \rho,\ 0 \le z \le l)$

$$E_z^{III}(\rho,z)=\frac{1}{j\omega\varepsilon_{III}}\sum_{n=0}^{n_3}d_nv_n^2H_0^{(2)}(v_n\rho)\cos\left(\frac{n\pi z}{l}\right)$$

$$H_\phi^{III}(\rho,z)=\sum_{n=0}^{n_3}d_nv_nH_1^{(2)}(v_n\rho)\cos\left(\frac{n\pi z}{l}\right)$$

iv) Region (IV,i), i=1 or 2, $(r_1 \le \rho \le b,\ p_{i-1}+h_{i-1} \le z \le p_i)$

$$E_z^{IV,i}(\rho,z)=\frac{1}{j\omega\varepsilon_{IV,i}}\sum_{n=0}^{n_{4,i}}\left(\alpha_n^{IV,i}\right)^2\left[e_n^{IV,i}H_0^{(1)}\left(\alpha_n^{IV,i}\rho\right)+f_n^{IV,i}H_0^{(2)}\left(\alpha_n^{IV,i}\rho\right)\right]\cos\left[\frac{n\pi\left(z-p_{i-1}-h_{i-1}\right)}{d_i}\right]$$

$$H_\phi^{IV,i}(\rho,z)=\sum_{n=0}^{n_{4,i}}\left(\alpha_n^{IV,i}\right)\left[e_n^{IV,i}H_1^{(1)}\left(\alpha_n^{IV,i}\rho\right)+f_n^{IV,i}H_1^{(2)}\left(\alpha_n^{IV,i}\rho\right)\right]\cos\left[\frac{n\pi\left(z-p_{i-1}-h_{i-1}\right)}{d_i}\right]$$

where $\gamma_n=\sqrt{\varepsilon_{rI}k_0^2-(n\pi/h)^2}$, $u_n=\sqrt{k_0^2-(n\pi/q)^2}$, $v_n=\sqrt{k_0^2-(n\pi/l)^2}$, and $\alpha_n^{IV,i}=\sqrt{\varepsilon_{rIV,i}\,k_0^2-(n\pi/d_i)^2}$. Especially, for $N=1$, $p_0=h_0=0$, $p_1=d_1$, $p_i=p_{i-1}+h_{i-1}+d_i$, and $p_{N+1}=h$. The unknown coefficients, a_n, b_n, c_n, d_n, e_n, and f_n can be obtained from matching boundary conditions at the interface between different regions, respectively.

III. Numerical Results and Verification

By assuming the excitation voltage, V_0 at the input port of coaxial cable and applying the matching boundary conditions, the derivation of simultaneous equation for the unknown coefficients in region I has been carried out as follows.

$$a_nH_0^{(1)}(\gamma_na)+b_nH_0^{(2)}(\gamma_na)=\frac{-j2\omega\varepsilon_IV_0\sin(n\pi d/h)}{\upsilon_n\gamma_n^2h(n\pi d/h)} \qquad (1)$$

In similar ways, the other simultaneous equations necessary for evaluating the unknown coefficients can be derived as follows.

i) For E – field at the interface between region I and IV

$$\frac{1}{\varepsilon_I}\gamma_n^2[a_n H_0^{(1)}(\gamma_n r_1)+b_n H_0^{(2)}(\gamma_n r_1)\upsilon_n h/2 =$$

$$\frac{1}{\varepsilon_{IV,1}}\sum_{n=0}^{n_{4,1}}\left(\alpha_n^{IV,1}\right)^2[e_n^{IV,1}H_0^{(1)}(\alpha_n^{IV,1}r_1)+f_n^{IV,1}H_0^{(2)}(\alpha_n^{IV,1}r_1)]I_{1nm}+$$

$$\frac{1}{\varepsilon_{IV,2}}\sum_{n=0}^{n_{4,2}}\left(\alpha_n^{IV,2}\right)^2[e_n^{IV,2}H_0^{(1)}(\alpha_n^{IV,2}r_1)+f_n^{IV,2}H_0^{(2)}(\alpha_n^{IV,2}r_1)]I_{2nm} \quad (2)$$

ii) For H – field at the interface between region I and IV,1

$$\sum_{n=0}^{n_1}\gamma_n[a_n H_1^{(1)}(\gamma_n r_1)+b_n H_1^{(2)}(\gamma_n r_1)]I_{3nm} =$$

$$\alpha_n^{IV,1}[e_n^{IV,1}H_1^{(1)}(\alpha_n^{IV,1}r_1)+f_n^{IV,1}H_1^{(2)}(\alpha_n^{IV,1}r_1)]\upsilon_n d_1/2 \quad (3)$$

iii) For H – field at the interface between region I and IV,2

$$\sum_{n=0}^{n_1}\gamma_n[a_n H_1^{(1)}(\gamma_n r_1)+b_n H_1^{(2)}(\gamma_n r_1)]I_{4nm} =$$

$$\alpha_n^{IV,2}[e_n^{IV,2}H_1^{(1)}(\alpha_n^{IV,2}r_1)+f_n^{IV,2}H_1^{(2)}(\alpha_n^{IV,2}r_1)]\upsilon_n d_2/2 \quad (4)$$

iv) For E – field at the interface between region II, IV and III

$$\frac{1}{\varepsilon_{II}}d_n v_n^2 H_0^{(2)}(v_n b)\upsilon_n l/2 =$$

$$\frac{1}{\varepsilon_{IV,1}}\sum_{n=0}^{n_{4,1}}\left(\alpha_n^{IV,1}\right)^2[e_n^{IV,1}H_0^{(1)}(\alpha_n^{IV,1}b)+f_n^{IV,1}H_0^{(2)}(\alpha_n^{IV,1}b)]I_{5nm}+$$

$$\frac{1}{\varepsilon_{IV,2}}\sum_{n=0}^{n_{4,2}}\left(\alpha_n^{IV,2}\right)^2[e_n^{IV,2}H_0^{(1)}(\alpha_n^{IV,2}b)+f_n^{IV,2}H_0^{(2)}(\alpha_n^{IV,2}b)]I_{6nm}$$

$$+\frac{1}{\varepsilon_{II}}\sum_{n=0}^{n_2}c_n u_n^2 J_0(u_n b)I_{7nm} \quad (5)$$

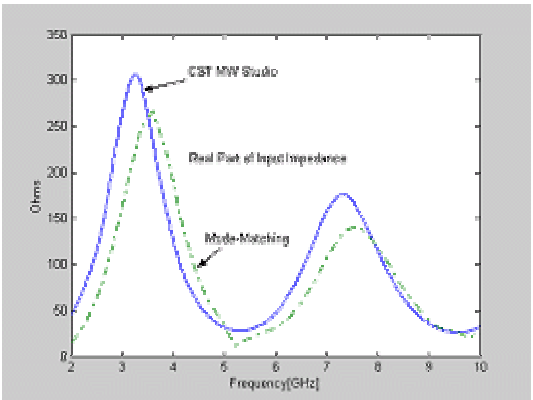

Fig. 3. The real part comparison of antenna input impedance between mode-matching analysis and a commercially available software ($b=3.11$, $h=31.75$, $N=0$, $l=1.54\lambda_0$, unit : [mm])

With the simultaneous equations shown in eqs. (1)~(5), additional boundary conditions necessary for uniquely solving the unknown modal coefficients are v) For H – field at the interface between region II and III, vi) For H – field at the interface between region IV, 1 and III, vii) For H – field at the interface between region IV, 2 and III. Fig. 3 and 4 describe the real part of antenna input impedances when the cases of $N=0$ and $N=1$ are considered. Except a little deviation at the peak point, two results obtained from our method and a commercially available software give a good agreement. The frequency shift in peak values can be overcome by increasing the number of mode assumed for the numerical calculations.

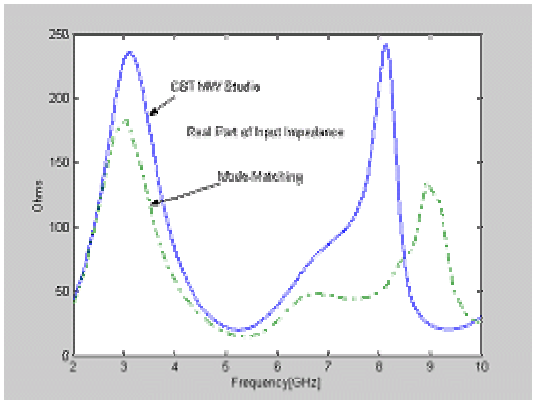

Fig. 4. The real part comparison of antenna input impedance between mode-matching analysis and a commercially available software
($b=3.11$, $h=31.75$, $N=1$, $l=1.54\lambda_0$, $h_1=13$, $r_1=b-0.79$, $p_1=d_1=d=1$, unit : [mm])

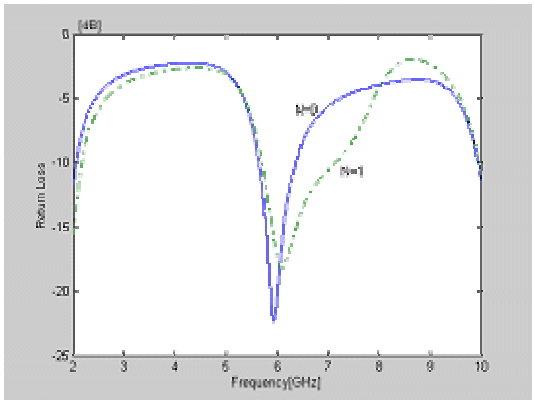

Fig. 5. A comparison of return loss according to the cases with($N=1$)/without($N=0$) horizontal parasitic strips of Fig. 1(a)

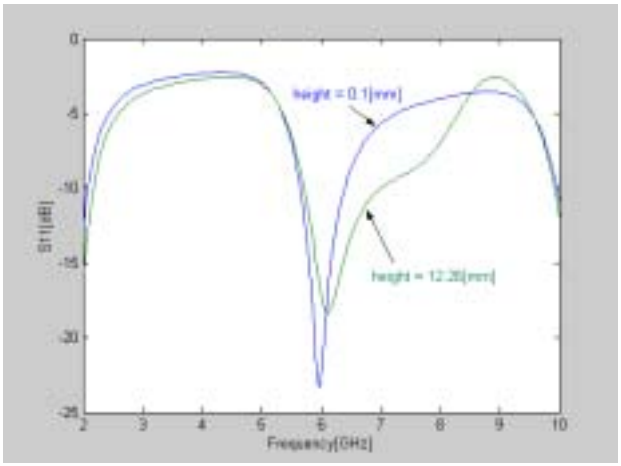

Fig. 6. A comparison of return loss according to the height of vertical parasitic strips ($N = 6$) of Fig. 1(b). The separation between the nearest strips is 20degrees.

Fig. 5 and 6 show that horizontal or vertical parasitic strips can be used for the enhancement of input impedance bandwidth of simple monopole antenna. Physically, the aim of loading circular disc on simple monopole antenna is to increase the area of radiator, leading to the shift of resonant frequency and an enhancement of input impedance bandwidth. In addition to that, in this paper, the parasitic strips around monopole antenna are suggested for the bandwidth extension near the resonant frequency. It is seen that the enhancement of impedance bandwidth can be accomplished by predicting the return loss according to the cases with ($N = 1$)/without ($N = 0$) parasitic elements. This phenomenon can be explained as a modification of current flows on main radiator due to additional inductances and capacitances caused by parasitic elements and main radiator.

IV. CONCLUSION

This paper deals with the bandwidth of input impedance and return loss loaded by horizontally and/or vertically attached parasitic strips around circular-disc loaded monopole antenna. In each region, the unknown modal coefficients have been obtained in numerically available series form. In addition to that, the numerical results carried out by our method have been compared with the data obtained from commercially available software for the clarity of our analysis. Finally, it is seen that the effect of attaching parasitic element on monopole antenna is to increase the bandwidth of return loss.

V. APPENDIX

$$I_{1nm} = (-1)^n \sin\left(\frac{m\pi d_1}{h}\right)\frac{m\pi/h}{(m\pi/h)^2-(n\pi/d_1)^2}$$

$$I_{2nm} = (-1)^m \sin\left(\frac{m\pi d_2}{h}\right)\frac{m\pi/h}{(m\pi/h)^2-(n\pi/d_2)^2}$$

$$I_{3nm} = (-1)^m \sin\left(\frac{n\pi d_1}{h}\right)\frac{n\pi/h}{(n\pi/h)^2-(m\pi/d_2)^2}$$

$$I_{4nm} = (-1)^n \sin\left(\frac{n\pi d_1}{h}\right)\frac{n\pi/h}{(n\pi/h)^2-(m\pi/d_2)^2}$$

$$I_{5nm} = (-1)^n \sin\left(\frac{m\pi d_1}{l}\right)\frac{m\pi/l}{(m\pi/l)^2-(n\pi/d_1)^2}$$

$$I_{6nm} = \left\{(-1)^n \sin\left(\frac{m\pi h}{l}\right) - \sin\left[\frac{m\pi}{l}(p_1+h_1)\right]\right\}\frac{m\pi/l}{(m\pi/l)^2-(n\pi/d_2)^2}$$

$$I_{7nm} = (-1)^m \sin\left(\frac{n\pi q}{l}\right)\frac{m\pi/l}{(m\pi/l)^2-(n\pi/q)^2}$$

REFERENCES

[1] C. A. Balanis, *Antenna Theory – Analysis and Design,* Second Edition, John Wiley & Sons, Inc., 1997.

[2] M. A. Morgan and F. K. Schwering, "Eigenmode analysis of dielectric loaded top-hat monopole antennas", *IEEE Trans. Antennas and Propagat.,* vol. AP-42, no. 1, pp. 54-61, Jan. 1994.

[3] Z. Shen and R. H. MacPhie, "Rigorous evaluation of the input impedance of a sleeve monopole by modal-expansion method", *IEEE Trans. Antennas and Propagat.,* vol. AP-44, no. 12, pp. 1584-1591, Dec. 1996.

[4] M. A. Morgan and R. C. Hurley, and F. K. Schwering, "Computation of monopole antenna currents using cylindrical harmonics", *IEEE Trans. Antennas and Propagat.,* vol. AP-38, no. 7, pp. 1130-1133, July 1990.

[5] L. A. Francavilla, J. S. McLean, H. D. Foltz, and G. E. Crook, "Mode-matching analysis of top-hat monopole antenna loaded with radially layered dielectric", *IEEE Trans. Antennas and Propagat.,* vol. AP-47, no. 1, pp. 179-185, Jan. 1999.

[6] H. Nakano, N. Ikeda, Y. W. Wu, R. Suzuki, H. Mimaki, and J. Yamauchi, "Realization of dual-frequency and wide-band VSWR performances using normal-mode helical and inverted-F antennas", *IEEE Trans. Antennas and Propagat.,* vol. AP-46, no. 6, pp. 788-793, June 1998.

[7] R. A. Abd-Alhameed and P. S. Excell, "Analysis of a normal-mode helical antenna including non-uniform wire surface current effects", *IEE Proc.-Microw. Antennas Propagat.,* vol. 146, no. 1, pp. 1-5, Feb. 1999.

[8] CST Microwave Studio, Release 5.0, Germany, 2005